Nonlinear radiative-condensation instability and pattern formation: One-dimensional dynamics

Igor Aranson and Baruch Meerson
Racah Institute of Physics, Hebrew University of Jerusalem, Jerusalem 91904, Israel

Pavel V. Sasorov
Institute of Theoretical and Experimental Physics, Moscow 117259, Russia
(Received 4 January 1993)

Nonlinear evolution of the radiative-condensation instability is investigated in the intermediate-wavelength limit, when the growth rate is maximal. The dynamics of a confined plasma is considered. This paper treats the planar geometry. Nonlinear reduced equations are derived for the instability, which account for the nonlocal feedback resulting from mass conservation and the finite size of the system. For a bistable heating-cooling function, it is shown that, in contrast to a number of previous studies where the isobaricity condition was employed, one-dimensional coherent patterns (spatial coexistence of two locally stable thermal equilibria, cool and hot) persist for a very long time.

PACS number(s): 52.35.Py, 95.30.Lz, 05.70.Fh

I. INTRODUCTION

Radiative condensations are generic phenomena intrinsic in optically thin plasmas subject to radiative cooling. They are often encountered in astrophysical, solar, and laboratory plasmas. Interstellar [1] and intergalactic [2] clouds, solar prominences [3], "marfes" in tokamaks [4], and many types of radiative contractions in laboratory gas discharges [5] represent relatively cool and dense plasma structures (patterns) which are surrounded by hot and rarefied plasmas and which strongly radiate. Alternatively, "bubbles" of hot and rarefied plasmas surrounded by cool and dense plasmas are frequently discussed in different astrophysical applications. Besides their astrophysical or applications-oriented interest, the coherent, strongly nonlinear patterns, forming from some "natural" initial conditions, represent an interesting example of self-organization in extended nonequilibrium media and deserve attention.

The radiative-condensation instability (RCI) has long been invoked as a mechanism for the formation of radiative condensations in various applications [6–8], and it has been extensively studied, analytically and numerically, starting from the pioneering work by Field [6]. The physics of the RCI is quite simple. Consider a uniform, optically thin plasma and assume that some external heating (for simplicity, uniform and constant in time) is balanced by radiative cooling. Suppose there is a local increase in the plasma density. Since the radiative cooling rate grows with the density, the temperature in this region starts to fall. In order to maintain constant pressure, plasma inflow starts, further increasing the density, and so on. If the perturbation size is too small, the perturbation is erased by heat conduction. Otherwise, the instability continues until a new equilibrium is reached.

The linear theory of the RCI has been developed quite adequately [6]. As for nonlinear analyses, they have been done numerically in many works, in the framework of full systems of nonlinear fluid dynamic (or magnetohydrodynamic) and thermal balance equations, one or two dimensional. The numerical simulations show that the instability is usually strong in the sense that it is not stabilized by weak nonlinearities, and the final state (often in the form of patterns) is very different from the initial one.

Simultaneously, attempts have been made to treat the nonlinear RCI analytically, and a number of sets of reduced nonlinear equations for the RCI were derived for different limiting cases. These models have provided a helpful physical insight into the nature of the instability. In a number of cases, informative analytical solutions have been obtained. Also, the reduced equations are much easier for numerical solution and subsequent interpretation. Finally, they have helped to find important similarities between the nonlinear RCI and other self-organization mechanisms.

The progress in analytical treatment is based on the explicit use of different time scales (and corresponding spatial scales) entering the problem. In the simplest case of an unmagnetized plasma with no external fields, these are the acoustic, radiative, and heat-conduction time scales. In the long-wavelength limit, the radiative time scale is the shortest, while the heat conduction is negligible. Then it appears that under certain conditions the RCI can be described by the fluid-dynamic equations with an "effective" pressure ensuring a "negative compressibility" of the gas over some range of densities [7,9,10]. If this range of densities is very large, one can formally extend the negative compressibility over the whole range of densities. In this case, the unstable gas flow was shown to develop, over a finite time internal, localized singularities [9], which can be interpreted as (a) very dense and cold states, and (b) very rarefied and hot states. These solutions were obtained in a planar geometry. In a three-dimensional (3D) geometry, the problem appears to be similar to the problem of the nonlinear gravitational instability, studied in many works (see [10] and references therein), and so the formation of flattened plasma con-

densations ("thermal pancakes") in the strongly nonlinear stage of the RCI was predicted [9]. Problems involving the alternating-sign compressibility and effects of heat conduction and viscosity in the long-wavelength limit of the RCI have been considered recently [11].

Most of the work on the RCI has been done, however, in the intermediate- and short-wavelength limits, when the acoustic time scale is the shortest one, the two limits differing in the role of heat conduction. In the intermediate-wavelength limit, the heat conduction is insignificant, at least in the beginning. This limit was considered by Sasorov [12] in a 3D geometry. Assuming isobaricity and choosing a model heating-cooling function with only one, unstable equilibrium, he showed that the formation of thermal pancakes, earlier predicted in the long-wavelength limit [9], persists in the intermediate-wavelength limit as well [12].

In the short-wavelength limit of the RCI, the heat conduction is important from the very beginning. The first consistent approach in this limit was taken, in a planar geometry, by Doroshkevich and Zel'dovich [13], although they considered the dynamics of a radiatively cooling conductive plasma without heating (that is, not in thermal equilibrium). Employing the isobaricity condition and transforming to the Lagrangian variables, they reduced the governing equations to a generalized reaction-diffusion equation (GRDE) for the plasma temperature. This equation was used to study the evolution of the interface between hot and cold gases (see also Ref. [14]). Doroshkevich and Zel'dovich studied different regimes of the interplay between the cooling and heat conduction and found different types of traveling temperature fronts, depending on the form of the cooling function. A similar planar GRDE in Lagrangian coordinates was derived by Meerson [15], who employed it in both the intermediate- and short-wavelength limits of the RCI. First, he used this equation to analyze the instability dynamics, starting from a small-amplitude, intermediate-wavelength perturbation around an unstable equilibrium. He showed that the first, radiative stage of the dynamics is completely determined by the form of the isobaric heating-cooling function and initial conditions. For the case of a bistable heating-cooling function (i.e., one with two stable thermal equilibria, adjacent to the unstable one), strong plasma stratification develops, and then heat conduction starts to act. Also, in the short-wavelength limit, a family of steady-state solutions in the form of standing nonlinear periodic temperature waves was found [15]; however, these solutions prove to be unstable for both periodic and no-flux boundary conditions. In the following, we shall limit ourselves to the case of the bistable heating-cooling function, frequently employed when studying the dynamics of the interstellar and intergalactic media. However, the set of reduced equations that we derive (see below) is valid for an arbitrary heating-cooling function.

Since reaction-diffusion equations of various forms have also arisen in numerous other contexts, a number of mathematically similar results were obtained in this field independently by many workers (see, e.g., [16–18] and references therein).

The problem of the long-time evolution of the strong planar plasma stratification, found in the intermediate-wavelength limit, was addressed in Ref. [19]. The same GRDE with periodic boundary conditions for the plasma temperature was used, and it was found that on a longer, heat-conduction-determined time scale, only one of the two locally stable thermal equilibria generally survives, the other one being a metastable state. Transition to the final uniform state occurs in the form of interaction between traveling temperature fronts which preserve their identity until "collision" and "annihilation." For a special value of the pressure, an individual temperature front is standing rather than moving [14,15,19]. In this case, the phase coexistence lasts for an exponentially long time and breaks down only because of the exponentially weak interaction between the neighboring fronts [20]. However, realization of this special case is highly unlikely in any natural isobaric environment.

Recently, the same one-dimensional GRDE has been used in the short-wavelength limit of the isobaric RCI [21]. It has been found numerically that, similar to the intermediate-wavelength limit, only one of the two stable uniform states finally survives for the no-flux boundary conditions.

The reason for this "uniformization" instability is superiority of the zero wave-number mode $k=0$ in the GRDE. Having the maximum growth rate, this mode normally wins the mode competition. The uniformization does not occur if prescribed temperatures and densities at the boundaries rather than the no-flux or periodic boundary conditions are specified. Such boundary conditions are frequently employed, for example, in the analysis of solar coronal plasma loops, bounded by much denser chromospheric plasma [22]. The prescribed boundary temperatures can eliminate the pattern-destroying $k=0$ mode and thus make steady patterns possible. However, in a number of one-dimensional numerical simulations employing the complete fluid dynamics and thermal balance equations, the no-flux boundary conditions were applied, and the formation of long-living coherent patterns was clearly observed [23]. Analyzing these simulations, one can see that the steady-state patterns do belong to the intermediate- or short-wavelength limit since their sizes are much less than the acoustic Field length $c_s\tau_r$, so that the plasma pressure can be assumed uniform (c_s is the acoustic velocity, τ_r is the characteristic radiative cooling time). However, the pressure can vary *in time*. Therefore, the following question arises: Is there a universal mechanism that would enable the unstable plasma to adjust its "floating" pressure properly and support long-living steady-state patterns, whose typical sizes are determined solely by the local plasma parameters and external heating rate? In a qualitative analysis of a similar system, McKee and Begelman [24] suggested that the answer to this question can be positive. In this paper we find the conditions for this suggestion to be correct in a one-dimensional system, and we develop a quantitative theory for the formation of long-lived patterns via the RCI. We consider a thermally bistable plasma, confined in a finite region of space by external forces (such as those produced by the average gravitational field

of stars in the Galaxy or, alternatively, sufficiently strong magnetic field, providing confinement of laboratory plasmas), and derive a set of reduced nonlinear equations for this system. This paper employs a planar geometry. We shall use the reduced equations to show that the nonlinear RCI develops coherent patterns which persist for a very long time. A subsequent paper will treat the two- and three-dimensional dynamics, where qualitatively new effects appear.

The present paper is organized in the following way. Section II contains the derivation of the 1D reduced equations for the nonlinear RCI. In Secs. III and IV we employ the reduced equations to analyze the radiative and conductive stages of the RCI, respectively. The reduced equations are solved numerically in Sec. V. Section VI contains a brief summary and discussion of the results.

II. REDUCED EQUATIONS

Let us consider a planar flow of an optically thin, ideal plasma of mass density ρ, temperature T, and velocity v, which is heated by some external agent and cooled radiatively. We are interested in the intermediate- and short-wavelength limits (the corresponding criteria are presented below), when the plasma pressure p is close to uniform. In this case the governing equations can be written in the following way [12,15]:

$$\frac{d\rho}{dt}+\rho\frac{\partial v}{\partial x}=0 , \tag{1}$$

$$\frac{1}{\gamma-1}\frac{dp}{dt}+\frac{\gamma}{\gamma-1}p\frac{\partial v}{\partial x}+\rho\mathcal{L}(\rho,T)-\frac{\partial}{\partial x}\left[K\frac{\partial T}{\partial x}\right]=0 , \tag{2}$$

$$\frac{\partial p}{\partial x}=0 , \tag{3}$$

$$p=\frac{R}{\mu}\rho T , \tag{4}$$

where $d/dt=\partial/\partial t+v\partial/\partial x$ is the total time derivative, $\mathcal{L}$ is the heating-cooling function (the difference between the rate of radiative cooling and the rate of heating per unit mass), $K=K(T)$ is the thermal conductivity, γ is the specific heat ratio, μ is the effective molar mass of the plasma, and R is the gas constant. The form of the function $\mathcal{L}(\rho,T)$ is determined by specific mechanisms of heating and cooling (see, e.g., Refs. [1,25–27] for the interstellar medium, quasar gas, solar corona, and tokamak plasma, respectively).

The simplest equilibria of the set (1)–(4) are $\rho=\rho_0=\text{const}$, $T=T_0=\text{const}$, $v=0$, and $\mathcal{L}(\rho_0,T_0)=0$. Linearizing Eqs. (1)–(4) around such an equilibrium, and looking for solutions in the form of $\exp(nt+ikx)$, we obtain

$$n=\frac{(\gamma-1)\mu}{\gamma R}\left[-\left[\frac{\partial\mathcal{L}}{\partial T_0}-\frac{\rho_0}{T_0}\frac{\partial\mathcal{L}}{\partial\rho_0}\right]-\kappa_0 k^2\right] , \tag{5}$$

where $\kappa_0=K(T_0)/\rho_0$ is the (unperturbed) thermal diffusivity. Of course, Eq. (5) coincides with the intermediate- and short-wavelength asymptotics of the general expression for the linear growth rate, found by Field [6]. It is seen from Eq. (5), that the radiative condensation mode is aperiodic, and the necessary condition for the instability is [6]

$$\left[\frac{\partial\mathcal{L}}{\partial T}\right]_p=\left[\frac{\partial\mathcal{L}}{\partial T}\right]_\rho-\frac{\rho}{T}\left[\frac{\partial\mathcal{L}}{\partial\rho}\right]_T<0 . \tag{6}$$

Thermal conduction always has a stabilizing effect, erasing perturbations with wavelengths shorter than some threshold one.

Being interested in the nonlinear evolution, we shall somewhat simplify the set (1)–(4). First, we assume that the temperature dependence of the heat conductivity is powerlike: $K(T)=K_0T^\alpha$, so that the cases of electron-dominated ($\alpha=\frac{5}{2}$) and neutral-dominated ($\alpha=\frac{1}{2}$) thermal conductivity can be accounted for properly. Instead of the plasma density, we introduce the specific volume $u(x,t)=\rho^{-1}(x,t)$ and eliminate the temperature $T(x,t)$, using the equation of state (4). Now the heating-cooling function $\mathcal{L}(\rho,T)=\mathcal{L}[u^{-1},(\mu/R)pu]$ depends on u and p. Introducing scaled variables $\hat{u}=u/u_0$ and $\hat{p}=p/p_0$, we define the dimensionless heating-cooling function $\lambda_E(\hat{u},\hat{p})$:

$$\frac{\gamma-1}{\gamma pu}\mathcal{L}\left[u^{-1},\frac{\mu}{R}pu\right]=\mathcal{L}_0\lambda_E(\hat{u},\hat{p}) , \tag{7}$$

where the parameters u_0 and p_0 and the coefficient $\mathcal{L}_0$ are chosen in such a way that the function $\lambda_E(\hat{u},\hat{p})$ evaluated, for example, at $\hat{u}=1$ and $\hat{p}=1$, is equal to unity. Following Begelman and McKee [28], we define the conductive Field length δ_F. In our notation,

$$\delta_F^2=\left[\frac{\mu}{R}\right]^{1+\alpha}\frac{(\gamma-1)K_0p_0^\alpha u_0^{1+\alpha}}{\gamma\mathcal{L}_0} . \tag{8}$$

δ_F shows the magnitude of the thermal conduction on the radiation time scale. Intermediate wavelengths are much longer than δ_F (however, much shorter than the acoustic Field length; see above), while short wavelengths are comparable to or smaller than δ_F.

Now we can introduce the remaining scaled variables: $\hat{x}=x/\delta_F$, $\hat{t}=\mathcal{L}_0t$, and $\hat{v}=v/(\delta_F\mathcal{L}_0)$, and rewrite Eqs. (1) and (2) in the following form:

$$\frac{\partial u}{\partial t}=u\frac{\partial v}{\partial x}-v\frac{\partial u}{\partial x} , \tag{9}$$

$$\frac{\dot{p}}{\gamma p}+\frac{\partial v}{\partial x}+\lambda_E(u,p)-p^\alpha\frac{\partial}{\partial x}\left[u^\alpha\frac{\partial u}{\partial x}\right]=0 , \tag{10}$$

where $\dot{p}\equiv dp/dt$ and the carets are omitted. Equations (9) and (10) must be supplemented by boundary conditions. The case of isobaricity $p=\text{const}$ corresponds to a prescribed, constant value of the pressure, necessarily the same at both boundaries. In this case Eqs. (9) and (10) reduce to those employed in Ref. [15]. Instead, we shall consider here a confined plasma and model this situation by putting the plasma in a one-dimensional "box" of fixed length L, so that the plasma velocity vanishes at both

boundaries. From this immediately follows mass conservation:

$$\int_0^L \frac{dx}{u(x,t)} = M = \text{const} . \tag{11}$$

It is natural to prescribe the no-flux boundary conditions for the density (or, equivalently, temperature), which lead to $\partial u/\partial x = 0$ at $x = 0$ and $x = L$. Then, integrating Eq. (10) over x from 0 to L, we arrive at the following relation:

$$\frac{\dot{p}}{\gamma p} = -\frac{1}{L}\int_0^L dx\, \lambda_E(u,p) , \tag{12}$$

which represents the evolution equation for the pressure and makes the set of reduced Eqs. (9), (10), and (12) closed. Equation (12) is very similar to the "global" pressure equation used by Begelman and McKee [28] for a qualitative analysis of the global effects of thermal conduction on "two-phase" media. Essentially, Eq. (12) corresponds to a particular limit of Begelman and McKee's analysis. They call this limit "isochoric" in the sense that "the mass is effectively contained within a fixed volume" [28]. We adopt a similar model of a confined two-phase plasma, but would rather call this limit "isochoric on the average." It should not be confused with the truly isochoric limit of thermal instability [6,29], which does not involve plasma motions and requires both the isochoric criterion $(\partial\lambda_E/\partial T)_u < 0$ and the strong inequality $k \ll (c_s\tau_r)^{-1}$. If the second condition is not satisfied, so that the characteristic wavelengths of the initial perturbation become comparable to the acoustic Field length, the isochoric criterion is irrelevant and plasma motions are important. Furthermore, if $k \gg (c_s\tau_r)^{-1}$, the instability develops as the RCI rather than the isochoric mode. We shall assume throughout the paper that the uniform thermal equilibria described by the heating-cooling function $\lambda_E(u,p)$ are isochorically stable.

Equations (9), (10), and (12) are also valid in the case of periodic boundary conditions, which makes them applicable for a $1D$ analysis of the RCI in tokamaks.

The reduced equations look simpler in Lagrangian coordinates. Introduce the (scaled) Lagrangian mass coordinate

$$m = \int_0^x \frac{dx}{u(x,t)} . \tag{13}$$

Then, transferring from variables x and t to the new variables m and t in Eqs. (9), (10), and (12), we arrive at the following two coupled equations:

$$\frac{\partial u}{\partial t} + \lambda_L(u,p) - p^{\alpha}\frac{\partial}{\partial m}\left[u^{\alpha-1}\frac{\partial u}{\partial m}\right] + \frac{u\dot{p}}{\gamma p} = 0 , \tag{14}$$

$$\frac{\dot{p}}{\gamma p} = -\frac{1}{L}\int_0^M dm\, \lambda_L(u,p) , \tag{15}$$

where $\lambda_L(u,p) = u\lambda_E(u,p)$, with the boundary conditions $\partial u/\partial m = 0$ at $m = 0$ and $m = M$.

Having found $u(m,t)$ and $p(t)$ from Eqs. (14) and (15), we can determine the plasma velocity

$$v(m,t) = \int_0^m \frac{\partial u}{\partial t} dm' = \frac{\partial}{\partial t}\int_0^m u\, dm' . \tag{16}$$

Finally, the relationship between Eulerian and Lagrangian coordinates, necessary for a transformation to Eulerian coordinates x and t, is given by

$$x(m,t) = \int_0^m u(m',t)dm' . \tag{17}$$

The mass conservation integral (11) looks trivial in the Lagrangian coordinates: $M = \text{const}$. On the other hand, the constancy of the "box" length, $L = \text{const}$, while trivial in the Eulerian coordinates, looks "nontrivial" in the Lagrangian coordinates:

$$\int_0^M u(m,t)dm = L = \text{const} . \tag{18}$$

For $p = \text{const} = 1$ (the "physical" pressure $p = p_0$), Eq. (14) reduces to the GRDE [13,15]:

$$\frac{\partial u}{\partial t} + \lambda_L(u,1) - \frac{\partial}{\partial m}\left[u^{\alpha-1}\frac{\partial u}{\partial m}\right] = 0 . \tag{19}$$

The reduced set of equations (9), (10), and (12) in the Eulerian coordinates or, alternatively, Eqs. (14) and (15) in the Lagrangian coordinates, are valid for any heating-cooling function. We shall concentrate in this paper on important case of a bistable heating-cooling function, widely employed when analyzing the interstellar and intergalactic gas dynamics [6–8,14,24,25,28]. For a fixed p, the bistable heating-cooling function $\lambda(u,p)$ (where λ means either λ_L or λ_E) has an "unstable" root $u_u(p)$, surrounded by two "stable" roots $u_1(p) < u_u(p)$ and $u_2(p) > u_u(p)$; see Fig. 1 (here stability or instability refers to the case of a zero heat conductivity). The signs of the derivatives $\partial u_1(p)/\partial p$, $\partial u_u(p)/\partial p$, and $\partial u_2(p)/\partial p$ can be established in the general case. Let us calculate $\partial u(p)/\partial p$ under the constraint $\lambda(u,p) = \text{const}$. We have

$$\left[\frac{\partial u(p)}{\partial p}\right]_{\lambda} = -\frac{(\partial\lambda/\partial p)_u}{(\partial\lambda/\partial u)_p} . \tag{20}$$

We have assumed that the uniform equilibria are *isochorically* stable: $(\partial\lambda/\partial T)_u \geq 0$ for $u = u_1$, u_u, and u_2. Using

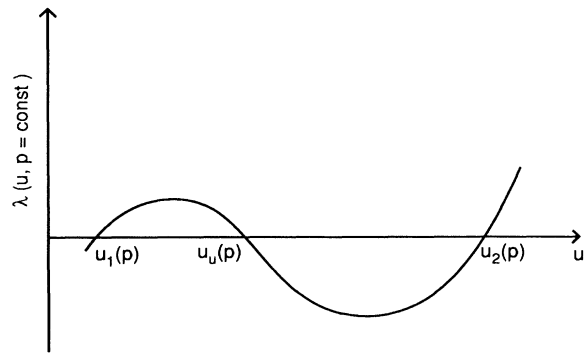

FIG. 1. A sketch of the bistable heating-cooling function $\lambda(u,p)$, calculated at a fixed uniform pressure. The root u_u is unstable with respect to the RCI, while the roots u_1 and u_2 are stable.

the equation of state (4), we see that the derivative $(\partial\lambda/\partial p)_u$, entering Eq. (20), is equal to $u(\partial\lambda/\partial T)_u$. Therefore, it is always non-negative, and we have $(\partial u(p)/\partial p)_\lambda \leq 0$ for the isobarically stable equilibria u_1 and u_2, and $(\partial u(p)/\partial p)_\lambda \geq 0$ for the isobarically unstable equilibrium u_u.

III. RADIATIVE STAGE

Let us assume that the initial condition $u(m,0)$ belongs to the intermediate-wavelength range and, as a first step, neglect conductivity. Let us compare the dynamics of the system (14) and (15) with those described by GRDE, Eq. (19). In the case of GRDE, if we start with an intermediate-wavelength perturbation $u(m,0)$ around the unstable root u_u =const so that $u(m,0)-u_u$ is of an alternating sign, the system will segregate, on a time scale of the order of unity (i.e., in several radiative cooling times in the dimensional variables), into regions occupied by the two stable phases with the specific volumes u_1 =const and u_2 =const [15] (we shall call them phase 1 and 2, respectively). (Note that in this and subsequent *order-of-magnitude estimates* we assume for convenience that neither of the roots u_1, u_u, and u_2 nor their differences are very large or small compared to unity, so that they do not introduce any additional time scales. This assumption can be obviously incorrect in applications, where thermal phases have temperatures and densities differing by two or more orders of magnitude [1–3]. In every such case the estimates should be worked out separately. Also, if the initial fluctuations of u around the unstable equilibrium are very small, the segregation time will obviously increase.)

In the framework of the GRDE, the stage of segregation, which we call radiative stage, is described by a simple implicit analytic solution [15] in the Lagrangian coordinates, which can be immediately obtained upon neglect of the conduction term in Eq. (19). The positions of the interphase boundaries, or fronts, in the Lagrangian coordinates coincide with the points where $u(m,0)=u_u$, and the fronts develop a zero thickness as $t\to\infty$. When the conduction is taken into account, the front width becomes of the order of δ_F [19].

System (14) and (15) is more complicated than the single partial differential equation (19), and even for zero conduction no analytic solution is generally possible. However, for a uniform initial condition $u(m,0)=u_0$, the analytic solution is simple and quite instructive. In this case, Eqs. (14) and (15) reduce to

$$\dot{u}=\lambda_L(u,p)\left[\frac{u}{u_0}-1\right], \tag{21}$$

$$\dot{p}=-\frac{\gamma p\lambda_L(u,p)}{u_0}. \tag{22}$$

It follows from Eq. (21) that the specific volume remains unchanged: $u(t)=u_0$. Then, assuming $u_1(p)<u_0<u_2(p)$ and using the inequality $[\partial u_u(p)/\partial p]_\lambda \geq 0$, we see from Eq. (22) that the gas pressure approaches the value p_r such that $u_u(p_r)=u_0$. In other words, at the radiative stage of the RCI the pressure adjusts itself so that an *arbitrary* uniform initial condition u_0 such that $u_1(p)<u_0<u_2(p)$ becomes an equilibrium. However, this uniform equilibrium is unstable with respect to *nonuniform* perturbations, which must lead to segregation. One can therefore assume that any nonuniform initial condition in Eqs. (14) and (15) with conduction neglected will also lead to segregation. In this sense, the segregation properties of the system (14) and (15) must be stronger than those of Eq. (19). Indeed, initial conditions such that $u(m,0)-u_0$ is less than zero (or, alternatively, larger than zero) everywhere do not cause segregation in GRDE [Eq. (19)], the whole system approaching the stable uniform state $u=u_1$ (correspondingly $u=u_2$). In contrast, neither of the uniform phases 1 and 2 is generally accessible in the system, described by Eqs. (14) and (15), because either of them would contradict integral (18). Instead, the pressure will have to change in such a way as to produce an alternating sign of the difference $u(m,t)-u_0(p)$ and therefore cause segregation.

Figure 2 gives a typical example of the radiative segregation, obtained by numerical solution of Eqs. (14) and (15) without the conduction term. In this example (and in other numerical simulations; see below) we chose the bistable heating-cooling function $\lambda_L(u,p)$ in the form of a cubic polynomial with respect to u:

$$\lambda(u,p)=[u-u_1(p)][u-u_u(p)][u-u_2(p)]. \tag{23}$$

The results presented in Fig. 2 were obtained for $u_1(p)=0.5/p$, $u_u(p)=p$, and $u_2(p)=2/p$. It is seen that a sharp front develops, the position of which does not coincide with the point where $u(m,0)=u_u$. Instead, the front position is determined now by both the initial condition and integral (18). For example, in the case of a single front, developing from a monotonic initial profile $u(m,0)$, the front position m_f is determined by the following relation:

$$m_f=\frac{u_2M-L}{u_2-u_1} \text{ or } m_f=\frac{L-u_1M}{u_2-u_1}, \tag{24}$$

depending on whether the function $u(m,0)$ is increasing or decreasing with m, respectively. In the Eulerian coordinates, the corresponding front positions in these two cases are $x_f=u_1m_f$ and $x_f=u_2m_f$, respectively. Note that the resulting specific volumes of the phases 1 and 2, entering Eq. (24), are determined by the final value of the plasma pressure. For the calculations presented in Fig. 2 we chose $M=50$ and the initial conditions $p(0)=1.0$ and $u(m,0)=1.05+0.4\cos(\pi m/M)$, so that the system length is $L=52.5$. The second relation in Eq. (24) correctly predicts the position of the developing front in the Lagrangian coordinates $m_f\approx 22.5$. In the Eulerian coordinates it corresponds to $x_f\approx 40.2$. In the case of two fronts, integral (18) predicts the distance between them.

We conclude this section by saying that in the first, radiative stage of the RCI, the thermally unstable plasma generally segregates into "cool drops" of phase 2 surrounded by the "hot gas" of phase 1 (or, alternatively, into "hot bubbles" of phase 1 surrounded by the "cool

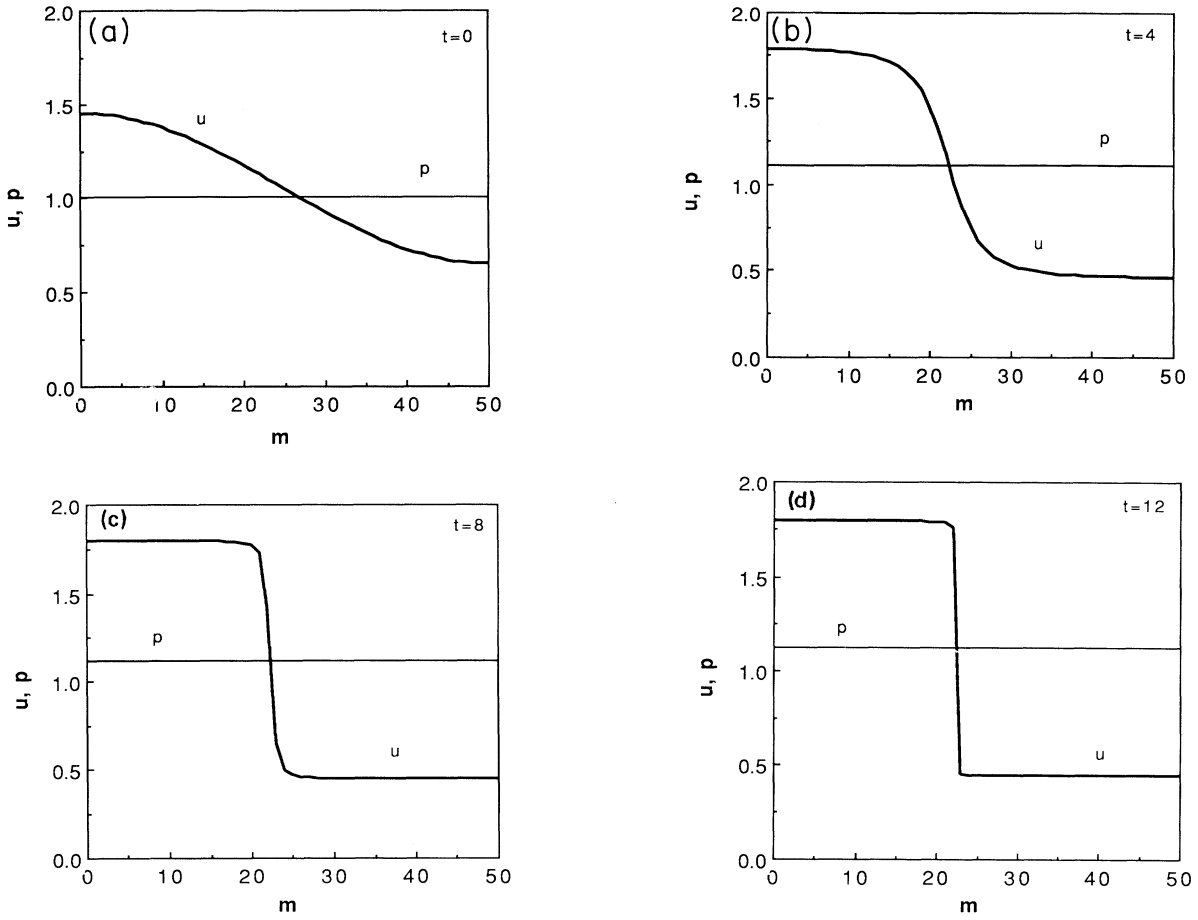

FIG. 2. An example of segregation, developing at the radiative stage of the RCI of a confined plasma. Equations (14) and (15) without the conduction term have been solved numerically for the bistable heating-cooling function $\lambda_L(u,p)$ from Eq. (23). Parameters are the following: $u_1=0.5/p$, $u_2=2/p$, $u_u=p$, and $M=50$. Shown are (a) initial conditions, $u(m,0)=1.05+0.4\cos(\pi m/M)$ and $p(0)=1.0$; (b)–(d) subsequent evolution of $u(m,t)$ and $p(t)$ for scaled times $t=4$, 8, and 12, respectively.

fluid" of phase 2). The slower conductive stage of the instability determines the final state of the system (evaporation of phase 2, condensation of phase 1, or their prolonged coexistence?) and requires a proper account of the heat conduction.

IV. CONDUCTIVE STAGE

We assume throughout this section that the size of the system is very large compared to the conductive Field length, that is, $L \gg 1$ in the scaled equations. Also, in the intermediate-wavelength limit, the front width, which is of the order of δ_F in "physical" units (and of the order of unity in the scaled variables; see below), is very small compared to the typical distance between the fronts. Finally, in a long system, a typical front is located very far from the system's boundaries. Then, until an exponentially large time (see Sec. VI), the form of the fronts and their dynamics can be investigated ignoring exponentially weak interactions between the fronts and the boundary effects. Therefore, an "elementary" object of the conductive stage is a slowly evolving single front, standing or moving. Our immediate aim is to exploit the strong inequality $L \gg 1$ and consider the statics and dynamics of the single front.

Let us return to Eqs. (9), (10), and (12) in Eulerian coordinates. (All the results in this section can be obtained in Lagrangian coordinates as well. However, we prefer to employ the Eulerian coordinates at this stage, since some of the following equations will also be used in the two- and three-dimensional cases, where Lagrangian coordinates become less convenient.) Let us look for an equilibrium $\partial/\partial t = v = 0$. We arrive at the following equation:

$$\frac{d}{dx}\left[u^{\alpha}\frac{du}{dx}\right]=p^{-\alpha}\lambda_E(u,p)\ , \tag{25}$$

which should be solved, in view of what is mentioned above, *for each front* under the following approximate boundary conditions: $u(x=-\infty)=u_1(p)$, $u(x=+\infty)=u_2(p)$, and $du/dx=0$ at both $-\infty$ and $+\infty$. When this solution is found, the alternative solution, for which $u(x=-\infty)=u_2(p)$ and $u(x=+\infty)=u_1(p)$, is obtained simply by putting $-x$ instead of x.

Multiplying Eq. (25) by $u^{\alpha}du/dx$, integrating it once,

and using the boundary conditions, we obtain

$$\frac{1}{2}\left[\frac{du}{dx}\right]^2 = u^{-2\alpha}p^{-\alpha}\int_{u_1(p)}^{u} u^{\alpha}\lambda_E(u,p)du \tag{26}$$

under condition

$$\int_{u_1(p)}^{u_2(p)} u^{\alpha}\lambda_E(u,p)du = 0 \ . \tag{27}$$

Generally, Eq. (27) can be satisfied only for some discrete values of p. For example, if $\lambda_E(u,p)$ has the form of a cubic polynomial (23) and $\alpha=0$, the values of p are the roots of the equation

$$2u_u(p)=u_1(p)+u_2(p) \ . \tag{28}$$

We assume that such a value of p is unique and denote it by p_*, so that we can replace p by p_* in the equilibrium relation (26). Now we obtain from Eq. (26) the equilibrium solution in the following form:

$$x+\text{const}=\left[\frac{p_*^{\alpha}}{2}\right]^{1/2}\int_{u_1}^{u}\frac{u'^{\alpha}du'}{\left[\int_{u_1}^{u'}\xi^{\alpha}\lambda_E(\xi,p_*)d\xi\right]^{1/2}} \ . \tag{29}$$

The equilibrium solution can be conveniently found in the particular case of the heating-cooling function (23) and $\alpha=0$:

$$u_*(x)=\frac{u_1+u_2}{2}+\frac{u_2-u_1}{2}\tanh\left[\frac{u_2-u_1}{2\sqrt{2p_*}}(x+\text{const})\right] ,$$

where u_1 and u_2 should be evaluated at $p=p_*$ from Eq. (28).

In the context of RCI, criterion (27) appeared in Refs. [14,15,19,20] and it represents the condition for a single front being standing rather than moving, thus making possible a prolonged two-phase coexistence. An equivalent criterion in the Lagrangian coordinates is obtained from Eq. (27) by replacing λ_E by λ_L/u. Equation (27) has also been encountered in the theory and numerous applications of the *reaction-diffusion equation,* where it is called "the area rule" (see [16–18] and references therein). In a natural *isobaric* system, realization of the special case described by the area rule is highly unlikely. On the contrary, we can assume that in confined plasmas with a "floating" pressure, the pressure can approach this special value p_* and make long-lived patterns possible. To verify this assumption, we shall consider first the slow motion of a *single* front, arising when the plasma pressure is close but not equal to the equilibrium pressure p_*: $p=p_*+\Delta p$, where $|\Delta p| \ll p_*$. Using the latter strong inequality, we can write

$$\lambda_E(u,p)\approx\lambda_E(u,p_*)+\mu(u)\Delta p \ , \tag{30}$$

where $\mu(u)=\partial\lambda_E(u,p)/\partial p$ calculated at $p=p_*$. We are looking for the traveling-wave solutions of Eqs. (9) and (10): $u(x,t)=u(\xi)$ and $v(x,t)=v(\xi)$, where $\xi=x-ct$, c is the front velocity. Equation (9) yields $v(\xi)=c+ju(\xi)$, where $j=\text{const}$ is the flux of material through the front in the reference frame where the front is at rest. We substitute this relation and Eq. (30) into Eq. (10) and obtain

$$j\frac{du}{d\xi}+\lambda_E(u,p_*)+\mu(u)\Delta p-p^{\alpha}\frac{d}{d\xi}\left[u^{\alpha}\frac{du}{d\xi}\right]=0 \ . \tag{31}$$

The term $(\gamma p_*)^{-1}(d\Delta p/dt)$ is of the next order of smallness (see below) and has therefore been neglected. Also, because of the smallness of j, we can replace $du/d\xi$ in the first term of Eq. (31) by its equilibrium value from Eq. (26). At this stage, we notice that using the quantity j is not very convenient, since, for a fixed front, the sign of j depends on our choice of the direction of the coordinate axis (or, alternatively, for a fixed coordinate axis, on the sign of $du/d\xi$). Instead, we can introduce the projection $j_n=\mathbf{j}\cdot\mathbf{n}$ of the flux vector $\mathbf{j}$ onto the unit vector $\mathbf{n}$, normal to the front and directed, for concreteness, from phase 1 to phase 2. In the planar case, which we are working with now, such a definition makes the subsequent equations independent of the sign of $du/d\xi$, which is quite convenient. Also, this definition becomes very convenient in the two- and three-dimensional cases, as will be seen in the subsequent paper [30].

Multiplying Eq. (31) by $u^{\alpha}du/d\xi$, integrating it over ξ from $-\infty$ to $+\infty$ and using the single-front boundary conditions and Eq. (27), we arrive at the following linear relation between j_n and the small pressure mismatch Δp:

$$j_n=-g\Delta p \ , \tag{32}$$

where

$$g=\frac{p_*^{\alpha/2}\int_{u_1}^{u_2}u^{\alpha}\mu(u)du}{\int_{u_1}^{u_2}\left[2\int_{u_1}^{u}\eta^{\alpha}\lambda_E(\eta,p_*)d\eta\right]^{1/2}du} \ . \tag{33}$$

Equation (32) implies that the flux of material from, say, phase 1 into phase 2 is the same for every front, as long as the fronts are sufficiently far from each other and from the boundaries. Defining the normal plasma velocity components in phases 1 and 2 and the normal component of the front velocity $\mathbf{c}$ in the same way as before, we have

$$v_{1n}=c_n-gu_1\Delta p \ , \quad v_{2n}=c_n-gu_2\Delta p \tag{34}$$

for phase 1 and 2, respectively.

The g factor in Eq. (33) can be calculated conveniently if we use the cubic polynomial (23) for λ_E and consider the case $\alpha=0$. The result is the following:

$$g=\frac{1}{\sqrt{2}}\left[2\frac{du_u}{dp}-\frac{du_1}{dp}-\frac{du_2}{dp}\right] , \tag{35}$$

which should be evaluated at $p=p_*$.

Now we shall use Eq. (32) to obtain the evolution equation for the pressure in the case of $|\Delta p| \ll p_*$. The pressure is changing because of the global dynamics of the system (global feedback); therefore we shall now consider the whole system, which pressure is already close to the equilibrium one $|\Delta p| \ll p_*$ and the mass transfer between neighboring regions occupied by phases 1 and 2 proceeds according to the local relation (32). Neglecting the front widths, we can write down the conditions of constancy of the system length and total mass:

$$L_1+L_2=L \ , \quad M_1+M_2=M \ , \tag{36}$$

where indices 1 and 2 correspond to the regions of phases 1 and 2, respectively. If N is the total number of fronts, then the net mass rate of "evaporation" is $dM_2/dt=j_nN$, while the net mass rate of "condensation" is $dM_1/dt=-j_nN$. Recalling that $L_1(t)=M_1(t)u_1(t)$ and $L_2(t)=M_2(t)u_2(t)$, using relations (32) and (36) and noticing that $du_{1,2}/dt=(\partial u_{1,2}/\partial p)_\lambda(dp/dt)$, we arrive at the following evolution equation for the pressure:

$$\frac{dp}{dt}=\frac{g(u_2-u_1)^2\langle u\rangle(p-p_*)}{\langle L\rangle\left[(u_2-\langle u\rangle)\dfrac{\partial u_1}{\partial p}+(\langle u\rangle-u_1)\dfrac{\partial u_2}{\partial p}\right]}, \tag{37}$$

where $\langle L\rangle=L/N$ is the average size of the spot occupied by any of the phases, while $\langle u\rangle=L/M=\text{const}$ is determined by the initial condition $u(x,0)$:

$$\langle u\rangle^{-1}=\frac{1}{L}\int_0^L\frac{dx}{u(x,0)}. \tag{38}$$

Generally, $u_{1,2}$ depend on p. In this case $\partial u_{1,2}/\partial p$ has been shown previously to be negative [see Eq. (20)]. The expressions g, $u_2-\langle u\rangle$, and $\langle u\rangle-u_1$ are all positive. Therefore, Eq. (37) predicts relaxation of the pressure to the equilibrium value $p\to p_*$. [Note that there is a degenerate case, in which both u_1 and u_2 are independent of the pressure, so that the right-hand side of Eq. (37) goes formally to infinity and the pressure relaxation time to zero. Actually, Eq. (37) is inapplicable in this case, and the relaxation time is of the order of the *radiative* time; see later.]

Equation (37) is valid in the Lagrangian coordinates as well. One should only use the simple relation between λ_L and λ_E: $\lambda_L=u\lambda_E$, when calculating the g factor from Eq. (33).

In deriving Eq. (37), we assumed that the number of fronts N is constant. In the beginning of the conductive stage, this assumption is generally not correct, and fast motions, "collisions" and "annihilations" of the fronts, occur (similar to the case of the GRDE [19]), so that irregularities in the pressure dynamics can be expected. However, towards the end of the conductive stage, when Δp is already sufficiently small, the front motion decelerates significantly and the assumption of a constant N becomes true as well, which makes the final pressure relaxation to p_* monotonic. Moreover, at this stage the quantities u_1, u_2, $\partial u_1/\partial p$, and $\partial u_2/\partial p$, entering Eq. (37), should be evaluated at $p=p_*$. As a result, the final pressure relaxation, described by Eq. (37), is always exponential in time: $\Delta p\propto\exp[-t/(C\langle L\rangle)]$, where the constant C is determined from Eq. (37). If neither large nor small factors are introduced by the roots of heating-cooling function, the constant C is of the order of unity, so that the (scaled) e-fold time of the pressure relaxation is of the order of $\langle L\rangle$, which is the large parameter of the theory.

Since the average distance between the fronts $\langle L\rangle$ proves to be an important characteristic of the dynamics, a few words seem to be in order on how to determine it. In simple cases, $\langle L\rangle$ is determined by the form of the Fourier spectrum of the initial perturbations. For example, if the Fourier spectrum has a pronounced maximum at some wavelength (belonging to the intermediate-wavelength limit), this wavelength will normally define $\langle L\rangle$. An extreme limit would be a monochromatic initial perturbation, like in Fig. 2, when $\langle L\rangle$ is simply equal to a half of the perturbation wavelength. On the contrary, if the initial perturbation spectrum has the form of a broadband noise with no preferential wave number, an *a priori* determination of $\langle L\rangle$ is difficult, and numerical solution of the reduced equations (9), (10), and (12) [or, alternatively, (14) and (15)] is required (see below).

So far, we have described the two-stage evolution of a thermally bistable, confined plasma and been able to show analytically (though for small pressure mismatches only) that the mass conservation and length constancy of the system do provide a universal mechanism of pattern formation: the plasma pressure approaches the special value p_*, for which the fronts stop and the patterns exist for a very long time. However, since the analytical theory is unable to describe the "violent" part of the conductive stage, when the pressure mismatches are still large, and fast front motions, collisions, and annihilations occur, we performed numerical simulations of the system's dynamics.

V. NUMERICAL SIMULATIONS

For the numerical simulations we employed the bistable heating-cooling function from Eq. (23) and solved numerically both the Eulerian equations (9), (10), and (12), and the Lagrangian equations (14) and (15).

For the Eulerian simulations we put $\alpha=0$ and $\gamma=\frac{5}{3}$ and chose $\lambda_E(u,p)$ from Eq. (23) with two sets of equilibria u_1, u_u, and u_2. The first set exemplified the nondegenerate case, when all the equilibria are p dependent. The second set corresponded to the degenerate case, when u_u depended on p, but u_1 and u_2 were constant. The boundary conditions were the same as above: $\partial u/\partial x=0$ at $x=0$ and L. The initial velocity was always taken to be zero.

For the first set of equilibria, we took $u_1=1/(2p)$, $u_u=p$, and $u_2=2/p$. In this case, the correct order of the equilibria, $u_1<u_u<u_2$, is provided at $1/\sqrt{2}<p<\sqrt{2}$, while the equilibrium pressure found from Eq. (28) is $p_*=\sqrt{5}/2$. The initial condition for the specific volume $u(x,0)$ had the form of a very small-amplitude broad-band noise with a zero average around some constant value $\langle u\rangle$, which belonged to the interval $[u_1(p),u_2(p)]$ for the initial value of the pressure $p(0)$. Note that the chosen initial condition included both intermediate- and short-wavelength Fourier components.

We performed a number of simulations, varying the system length and the initial conditions for the specific volume and pressure. A typical example of the nonlinear dynamics of the RCI is shown in Fig. 3, where the profile of the specific volume of the plasma is presented at four successive moments in time: 16, 30, 40, and 300, and in Fig. 4, where the pressure evolution is shown, starting from the initial values $\langle u\rangle=0.8$ and $p(0)=1.0$. The (scaled) total length of the system L was taken to be 150. The (scaled) total mass of the gas was therefore $M=\frac{150}{0.8}=187.5$. It is seen that in the beginning the pres-

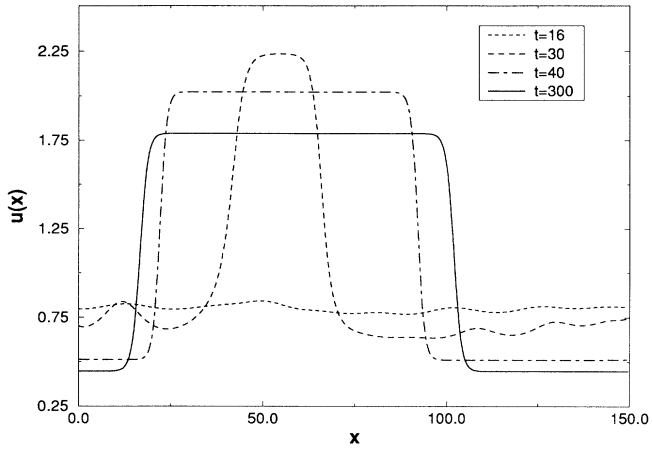

FIG. 3. Development of steady-state patterns in the process of nonlinear RCI (nondegenerate case). Shown is the spatial profile of the specific volume $u(x,t)$, found by the numerical solution of Eqs. (9), (10), and (12), vs time. The heating-cooling function $\lambda_E(u,p)$ is taken from Eq. (23) with $u_1=0.5/p$, $u_2=2/p$, $u_u=p$; parameter $\alpha=0$ and $\gamma=5/3$. The initial condition for $u(x,t)$ represents broadband noise with a very small amplitude around 0.8; the initial velocity is zero, the initial pressure is 1.0. The evolution is shown in four successive (scaled) time moments: 16 (short dashes), 30 (medium dashes), 40 (long and short dashes), and 300 (solid line).

sure rapidly "jumps down" to $\langle u \rangle = 0.8$. In other words, the initial condition for the specific volume *becomes* a small perturbation around an unstable equilibrium, as predicted by the "uniform" equations (21) and (22). Then the linear stage of the RCI starts. The perturbations with too short wavelengths are strongly damped in agreement with Eq. (5), so that they are already absent in Fig. 3. (Noteworthy in this stage is the U-shaped valley around $t=15$ in Fig. 4. It is explained by the fact that pressure variations vanish in the linear theory with respect to u and v, and appear only in the second order in the perturbation amplitudes.) After that the instability develops nonlinearly causing segregation (around $t=30$), while the plasma pressure rapidly grows. Since the initial perturbation amplitudes are very small in this example, the radiative stage takes a somewhat longer time. After a transient process, a steady coherent pattern forms, which consists of a lower-density, higher-temperature bubble, surrounded by two higher-density, lower-temperature drops. The equilibrium phase boundaries represent two symmetric fronts, described in the beginning of Sec. IV. The pattern reaches its steady state around $t=80-100$. The distance between the fronts coincides with that predicted by the length and mass conservation (the total mass was preserved by our numerical scheme up to the sixth digit after the decimal point). The plasma pressure finally relaxes monotonically to a value very close to $p_*=\sqrt{5}/2\approx 1.12$, as predicted by the theory. For larger scaled times (up to $t=300$) the profile of u and the plasma pressure do not show any change. We compared the final stage of the pressure relaxation, found numerically, with that predicted by Eq. (37). To this end, we calculated the coefficients entering Eq. (37) for the chosen $\lambda_L(u,p)$, evaluating them at $p=p_*=\sqrt{5}/2$. Equation (35) for the g factor gives $g=2\sqrt{2}$. The only quantity that cannot be found analytically is the final number of fronts; therefore we took it from the numerical results: $N=2$, which gives $\langle L \rangle = \frac{150}{2}=75$. Substituting all the coefficients into Eq. (37), we obtain $dp/dt \approx -0.057(p-p_*)$, so that the theoretical prediction of the relaxation rate is 0.057. Figure 5 shows, on a logarithmic scale, the final stage of the pressure relaxation found numerically, and its linear approximation. It is seen that the relaxation is indeed exponential, starting from $t\approx 50$. The relaxation rate found numerically is approximately 0.058, so that the theory predicts the relaxation rate with a very good accuracy.

For the second set of equilibria (degenerate case) we used $u_u=p$ and different constant values of u_1 and u_2. Figures 6 and 7 show an example of the dynamics of the RCI for $u_1=0.5$ and $u_2=2.0$. This time we started with $t=0$ to show the initial condition for the specific volume:

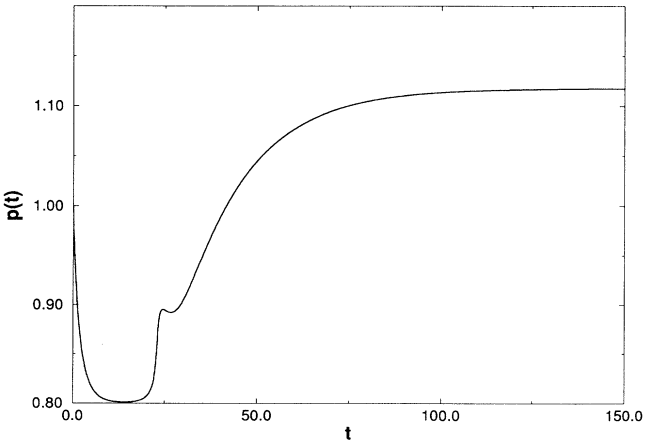

FIG. 4. Plasma pressure vs time corresponding to Fig. 3.

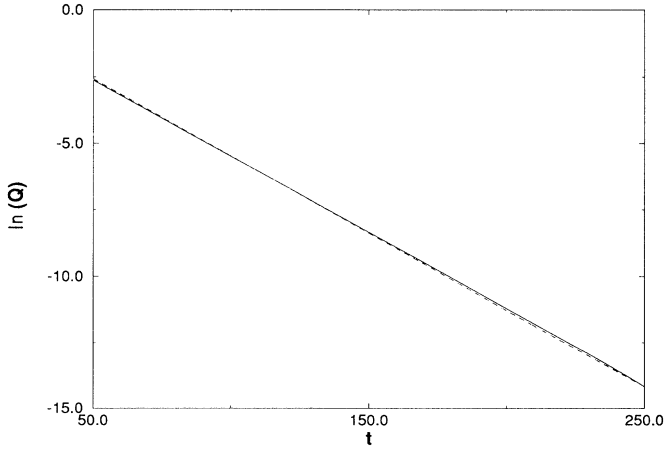

FIG. 5. Final pressure relaxation corresponding to Fig. 4. Shown are the natural logarithm of Q (where Q is the absolute value of the difference between the pressure and its equilibrium value $p_*=\sqrt{5}/2$) vs time and its linear approximation.

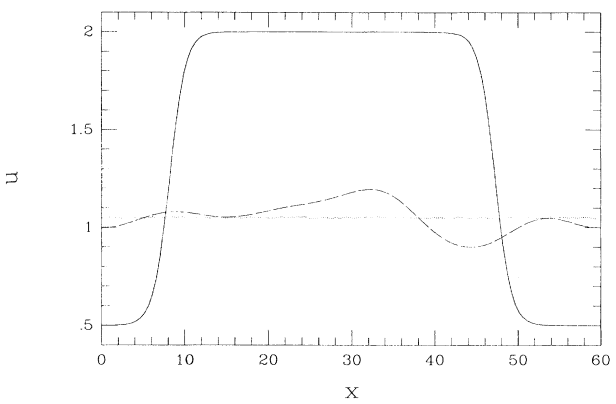

FIG. 6. Development of steady-state patterns in the process of nonlinear RCI (degenerate case). Shown is the spatial profile of the specific volume $u(x,t)$, found by the numerical solution of Eqs. (9), (10), and (12), vs time. The heating-cooling function $\lambda_E(u,p)$ is taken from Eq. (23) with $u_1=0.5$, $u_2=2.0$, $u_u=p$; parameter $\alpha=0$ and $\gamma=5/3$. The initial condition for $u(x,t)$ represents a small-amplitude broadband noise around 1.05. The initial pressure is 1.05; the initial velocity is zero. The evolution is shown in three successive (scaled) moments of time: 0 (dotted line), 10 (short dashes), and 200 (solid line).

a small-amplitude broadband noise around the unstable equilibrium $u_u[p(0)]$. The results are very similar to those found in the nondegenerate case: damping of short-wavelength perturbations, radiative segregation, and development of a long-lived steady pattern due to relaxation of the pressure to the special value p_* [in this case $p_*=(u_1+u_2)/2=1.25$]. Again, the distance between the fronts is determined by the length and mass conservations. However, there is an important difference in the final pressure relaxation dynamics. It is seen from Figs. 6 and 7 that the relaxation time in this case is of the order of the *radiative* time. Also noteworthy in Fig. 7 is the pronounced "overshoot" before the final pressure relaxation. This overshoot was seen in every numerical run with constant u_1 and u_2, and it was normally absent in nondegenerate cases.

For the numerical solution of the Lagrangian equations (14) and (15), we took $\alpha=1$ (a model thermal diffusivity,

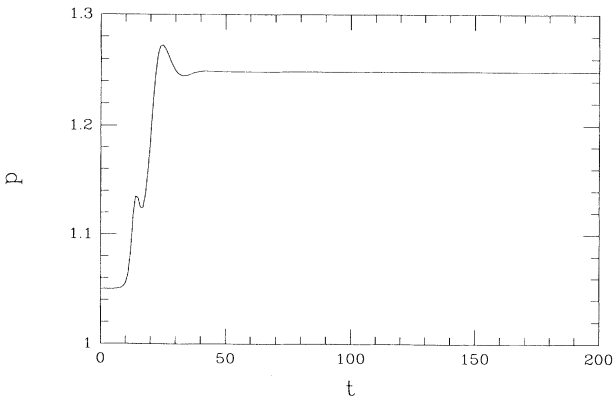

FIG. 7. Plasma pressure vs time corresponding to Fig. 6.

proportional to the temperature) and chose the heating-cooling function $\lambda_L(u,p)$ from Eq. (23) (that is, a heating-cooling function *different* from that in the previous example). We performed simulations with different sets of equilibria and different initial conditions. We do not present these results here because they closely resemble those shown in Figs. 3–7. We always observed formation of long-lived patterns, accompanied by pressure relaxation to the special value determined by the "area rule" for a single front.

VI. SUMMARY AND DISCUSSION

We have considered the nonlinear dynamics of the radiative condensation instability in a planar geometry. We have found a universal mechanism, by which long-lived coherent patterns develop in the process of the instability. This mechanism is provided by a global feedback in the instability dynamics, resulting from the mass conservation and constancy of the system length, which are natural for plasmas confined by external forces. The global feedback makes a thermally bistable plasma relax to a strongly nonuniform equilibrium, representing coexistence of the two phases: cool and dense, and hot and rarefied. This coherent two-phase equilibrium becomes possible because the plasma pressure approaches the special value for which individual fronts separating the phases become standing rather than moving. Numerical simulations strongly support and even reinforce our theoretical predictions, eliminating the limitation of small pressure mismatches used in the theory.

In the nondegenerate case, when all the equilibria are pressure dependent, the dynamics of the confined, thermally bistable plasma consists of two main stages. During the first radiative stage, the duration of which is determined by the radiative cooling time (and is the order of 10 in our scaled examples), the plasma segregates into two thermal phases with sharp boundaries (fronts) between them. The plasma pressure varies significantly during this stage. The mass ratio of the two phases, the number and location of homogeneous spots in each of them, and the gas pressure at the end of the radiative stage depend on the initial conditions. Then the much slower conductive stage starts, when the phase interfaces (fronts) move with velocities of the order of $\delta_F\mathcal{L}_0$ (which is unity in the scaled equations). Some of the fronts can collide and annihilate, leading to irregular pressure dynamics. At the end of the conductive stage, the fronts steadily decelerate and finally stop, with p approaching p_* exponentially. This implies development of a long-lived stratification or pattern formation via the RCI. A typical duration of the second phase is of the order of the average distance between the fronts, divided by the typical front speed. In the scaled units, the duration is of the order of $\langle L \rangle$, which is the large parameter of the theory. It is important that, for a given heating-cooling function, the equilibrium ratio of masses of the two phases, which sets in at the end of the conductive stage, depends only on the total plasma mass and the system length. The equilibrium plasma pressure, developing towards the end

of the conductive stage, is determined by the "area rule" and depends only on the form of the heating-cooling function.

In the previous isobaric studies of the nonlinear RCI long-lived nonuniform equilibria were found only when the special value of the plasma pressure was prescribed by the boundary conditions, which is very unlikely. Besides, if the pressure of an isobaric system slightly deviates from the special value, a slow front motion will start. The front speed will be only linearly small with the pressure deviation, so that the characteristic time for the erosion of patterns in the isobaric case will be inversely proportional to the pressure deviation (and directly proportional to the large parameter $\langle L \rangle$ [19]). In contrast, in a confined plasma with a "floating" pressure, the lifetime of the patterns is *exponentially* large with respect to the large parameter $\langle L \rangle$, *no matter what the initial pressure is.*

An interesting question concerns the *final,* third stage of the development of the RCI, when the weak interfront interaction and boundary effects become important. The question is of academic interest for sufficiently large systems (such as many interstellar clouds). However, for smaller systems (closer to the short-wavelength limit), this stage can become attainable. The present work has not addressed this question, but we can make some simple predictions, which have to be elaborated in the future. First, because of the mass conservation, no complete "uniformization" is possible at the third, "superlong" stage, in contrast to the isobaric case, considered recently [20]. Therefore, some (at least elementary) pattern structure must exist "forever." On the other hand, a family of *exact* equilibrium solutions of Eq. (25) in an unbounded medium exists, which represent nonlinear periodic standing temperature (and density) waves [15]. Solutions, consisting of an integer number of "segments" of such temperature waves and satisfying the no-flux boundary conditions, can always be constructed, unless the system is too short. These solutions provide *all* possible candidates for the final state, and one can assume that the "simplest" of them, containing only one front, will generally be stable and, therefore, realizable as $t \to \infty$. The expected (scaled) duration of the third stage must be of the order of $\exp L$, which is exponentially large with respect to the ratio of the system length to the conductive Field length, the large parameter of the theory.

As has been noted earlier, we assumed that the roots u_1, u_u, and u_2 of the heating-cooling function do not introduce large or small parameters into the theory. In many applications this assumption can be violated. For example, if $u_2 \gg u_u$, the electron heat conduction (which grows with the temperature like $T^{5/2}$) can become important *before* the full phase segregation develops. Such cases should be analyzed separately within the framework of the reduced equations.

In the two- or three-dimensional case, the conductive stage becomes more complex, as a new factor, the front curvature, affects the dynamics. This and related problems will be treated in a subsequent paper [30].

ACKNOWLEDGMENTS

This work was initiated when one of the authors (P.S.) visited the Racah Institute of Physics, the Hebrew University of Jerusalem. We are very grateful to the Racah Institute for the support, which helped to make this visit possible. The work was completed when another author (B.M.) visited the Solar Theory Group, Department of Mathematical and Computational Sciences, University of St. Andrews. He is very grateful to the Group staff, and especially to E. R. Priest for their hospitality. This work was supported, in part, by a Soros Foundation grant from the American Physical Society and by the Wolfson Family Trust and Alexander-von-Humboldt Foundation.

[1] L. Spitzer, *Physical Processes in the Interstellar Medium* (Wiley, New York, 1978); S. A. Kaplan and S. B. Pikel'ner, *Physics of the Interstellar Medium* (Nauka, Moscow, 1979) (in Russian).

[2] K. Davidson, Astrophys. J. **171**, 213 (1972).

[3] E. Tandberg-Hanssen, *Solar Prominences* (Reidel, Dordrecht, 1974).

[4] J. L. Terry, E. S. Marmar, and S. M. Wolfe, Bull. Am. Phys. Soc. **26**, 886 (1981).

[5] A. V. Nedospasov and V. D. Khait, *Oscillations and Instabilities of a Low-Temperature Plasma* (Nauka, Moscow, 1978) (in Russian).

[6] G. B. Field, Astrophys. J. **142**, 531 (1965).

[7] S. B. Pikel'ner, Astron. Zh. **44**, 915 (1967) [Sov. Astron. **11**, 737 (1968)].

[8] G. B. Field, D. W. Goldsmith, and H. J. Habing, Astrophys. J. Lett. **155**, L149 (1969).

[9] B. I. Meerson and P. V. Sasorov, Zh. Eskp. Teor. Fiz. **92**, 531 (1987) [Sov. Phys.—JETP **65**, 300 (1987)].

[10] Ya. B. Zel'dovich and I. D. Novikov, *The Structure and Evolution of the Universe, Relativistic Astrophysics, Vol. 2* (University of Chicago Press, Chicago, 1983).

[11] B. Meerson, C. D. C. Steele, A. M. Milne, and E. R. Priest, Phys. Fluids B (to be published).

[12] P. V. Sasorov, Pis'ma v Astron. Zh. **14**, 306 (1988) [Sov. Astron. Lett. **14**, 129 (1988)].

[13] A. G. Doroshkevich and Ya. B. Zel'dovich, Zk. Eksp. Teor. Fiz. **80**, 801 (1981) [Sov. Phys.—JETP **53**, 405 (1981)].

[14] Ya. B. Zel'dovich and S. B. Pikel'ner, Zh. Eksp. Teor. Fiz. **56**, 310 (1969) [Sov. Phys.—JETP **29**, 170 (1969)].

[15] B. Meerson, Astrophys. J. **347**, 1012 (1989).

[16] D. A. Frank-Kamenetskii, *Diffusion and Heat Transfer in Chemical Kinetics* (Plenum, New York, 1969).

[17] P. Fife, *Mathematical Aspects of Reacting and Diffusing Systems,* Lecture Notes in Biomathematics Vol. 28 (Springer-Verlag, New York, 1979).

[18] J. D. Murray, *Mathematical Biology* (Springer-Verlag, Berlin, 1989).

[19] A. M. Dimits and B. Meerson, Phys. Fluids B **3**, 1420 (1991).

[20] C. Elphick, O. Regev, and N. Shaviv, Astrophys. J. **392**, 106 (1992).

[21] B. Meerson and N. Persky (private communication).

[22] R. J. Bray, L. E. Cram, C. J. Durrant, and R. E. Loughhead, *Plasma Loops in the Solar Corona, Cambridge Astrophysics Series, Vol. 18* (Cambridge University Press, Cambridge, 1991).
[23] E. S. Oran, J. T. Mariska, and J. P. Boris, Astrophys. J **254**, 349 (1982); D. McCarthy and J. F. Drake, Phys. Fluids B **3**, 22 (1991).
[24] C. F. McKee and M. C. Begelman, Astrophys. J. **358**, 392 (1990).
[25] S. Lepp, R. McCray, J. M. Shull, D. T. Woods, and T. Kallman, Astrophys. J. **288**, 58 (1985).
[26] E. R. Priest, *Solar Magnetohydrodynamics* (Reidel, Dordrecht, 1982).
[27] T. E. Stringer, in *Proceedings of the 12th European Conference on Controlled Fusion and Plasma Physics, Budapest, Hungary* (European Physical Society, Geneva, 1985), Part 1, p. 86.
[28] M. C. Begelman and C. F. McKee, Astrophys. J. **358**, 375 (1990).
[29] E. N. Parker, Astrophys. J. **117**, 431 (1953).
[30] I. Aranson, B. Meerson, and P. V. Sasorov (unpublished).